Fundamental ICRF heating of deuterium ions in JET-DTE2

Lerche, E.; Maslov, M.; Jacquet, Ph; Monakhov, I.; King, D.; Keeling, D.; Challis, C. D.; Eester, D. Van; Mantica, P.; Maggi, C.

Total number of authors:
52

Published in:
AIP Conference Proceedings

Link to article, DOI:
10.1063/5.0162554

Publication date:
2023

Document Version
Publisher's PDF, also known as Version of record

RESEARCH ARTICLE | AUGUST 18 2023

Fundamental ICRF heating of deuterium ions in JET-DTE2

E. Lerche ✉; M. Maslov; Ph. Jacquet; I. Monakhov; D. King; D. Keeling; C. D. Challis; D. Van Eester; P. Mantica; C. Maggi; J. Garcia; F. Auriemma; R. Coelho; I. Coffey; A. Chomiczewska; E. Delabie; R. Dumont; P. Dumortier; J. Eriksson; J. Ferreira; M. Fitzgerald; M. Fontana; Z. Ghani; N. Hawkes; J. Hobirk; Ph. Huynh; T. Johnson; A. Kappatou; Y. Kazakov; V. Kiptily; K. Kirov; M. Lennholm; E. de la Luna; J. Mailloux; M. Marin; G. Matthews; S Menmuir; J. Mitchell; M. Nocente; J. Ongena; A. Patel; G. Pucella; E. Rachlew; D. Rigamonti; F. Rimini; S. Silburn; P. Siren; M. Salewski; E. Solano; Z. Stancar; M. Tardocchi; M. Valisa; JET contributors

AIP Conf. Proc. 2984, 030005 (2023)
https://doi.org/10.1063/5.0162554

Fundamental ICRF Heating of Deuterium Ions in JET-DTE2

E. Lerche[1,2,a], M. Maslov[1], Ph. Jacquet[1], I. Monakhov[1], D. King[1], D. Keeling[1], C. D. Challis[1], D. Van Eester[2], P. Mantica[3], C. Maggi[1], J. Garcia[1,4], F. Auriemma[5], R. Coelho[6], I. Coffey[1,7], A. Chomiczewska[8], E. Delabie[9], R. Dumont[4], P. Dumortier[1,2], J. Eriksson[10], J. Ferreira[6], M. Fitzgerald[1], M. Fontana[11], Z. Ghani[1], N. Hawkes[1], J. Hobirk[12], Ph. Huynh[4], T. Johnson[13], A. Kappatou[12], Y. Kazakov[2], V. Kiptily[1], K. Kirov[1], M. Lennholm[1], E. De la Luna[14], J. Mailloux[1], M. Marin[11], G. Matthews[1], S Menmuir[1], J. Mitchell[1], M. Nocente[3], J. Ongena[2], A. Patel[1], G. Pucella[15], E. Rachlew[16], D. Rigamonti[3], F. Rimini[1], S. Silburn[1], P. Siren[1], M. Salewski[17], E. Solano[14], Z. Stancar[1,18], M. Tardocchi[3], M. Valisa[5] and JET contributors

[1] UKAEA, Culham Science Centre, Abingdon, Oxon, OX14 3DB, UK
[2] Laboratory for Plasma Physics, ERM/KMS, B-1000 Brussels, Belgium
[3] Institute of Plasma Science and Technology, CNR, 20125 Milano, Italy
[4] CEA, IRFM, F-13108 St-Paul-Lez-Durance, France
[5] Consorzio RFX ISTP-CNR , 35127 Padova, Italy
[6] IPFN, Instituto Superior Tecnico, Universidade de Lisboa, 1049-001 Lisbon, Portugal
[7] Queen's University, BT7 1NN Belfast, United Kingdom
[8] Institute of Plasma Physics and Laser Microfusion, Hery 23, 01-497 Warsaw, Poland
[9]Oak Ridge National Laboratory, Oak Ridge, Tennessee, 37830 USA
[10] Department of Physics and Astronomy, Uppsala University, 75120 Uppsala, Sweden
[11] EPFL, Swiss Plasma Center (SPC), CH – 1015 Lausanne, Switzerland
[12] Max-Planck-Institut für Plasmaphysik, Boltzmannstr. 2, 85748 Garching, Germany
[13]Fusion Plasma Physics, EES, KTH, SE-10044 Stockholm, Sweden
[14] Laboratorio Nacional de Fusión, CIEMAT, 28040 Madrid, Spain
[15] ENEA, Fusion and Nuclear Safety Department, C.R. Frascati, 00044 Frascati, Italy
[16] Department of Physics, KTH, 10396 Stockholm, Sweden.
[17] Technical University of Denmark, DTU, 2800 Kongens Lyngby, Denmark
[18] Slovenian Fusion Association (SFA), Jozef Stefan Institute, SI-1000 Ljubljana, Slovenia

[a)]Corresponding author: Ernesto.Lerche@ukaea.uk

Abstract. Beam-target reactions are responsible for a substantial fraction of the fusion power generated in D-T plasmas in JET-ILW (Be/W-wall), with ion temperatures of 10-12keV and large neutral-beam injection (NBI) power. It is known that injecting D beam ions with energies of ~100-150keV in T-rich plasmas has a larger potential for beam-target fusion than in 50:50 D:T plasmas, but such a scenario was never developed in the past D-T experiments performed in JET-C (Carbon-wall) and in TFTR in the 90's. On top of the intrinsic advantages of using D beams in T-rich plasmas for D-T neutron production, simulations have shown that fundamental ion-cyclotron resonance heating (ICRH) of the D ions can significantly boost the net fusion reactivity, since both the thermalized D ions and the fast D-NBI ions are accelerated to energy ranges that are optimal for the D-T reaction cross-section. The beneficial effect of fundamental D ICRH on thermal D minorities in tritium plasmas (without NBI) was identified in the JET-C D-T experiments, but was not tested in high performance H-mode discharges with D-NBI heating. In 2021, dedicated JET-ILW DTE2 [1] experiments confirmed - for the first time - the improved fusion performance of T-rich plasmas with high D-NBI power and highlighted the key impact of fundamental D ICRH on the fusion reactivity. This new scenario lead to the world-wide 5s averaged fusion power (and energy) record in D-T tokamak plasmas with dominant beam-target reactions. A brief experimental overview followed by detailed RF wave / Fokker-Planck simulations including NBI-ICRH synergy will be presented, to disentangle the different components contributing to the high neutron yield achieved in these experiments.

24th Topical Conference on Radio-frequency Power in Plasmas
AIP Conf. Proc. 2984, 030005-1–030005-10; https://doi.org/10.1063/5.0162554
Published by AIP Publishing. 978-0-7354-4604-5/$30.00

INTRODUCTION

ITER and future fusion reactors rely on reaching high enough plasma temperatures for thermonuclear fusion reactions between the bulk fuel ions – Deuterium and Tritium - to occur. Even if a substantial amount of Neutral Beam ions is injected in the plasma, their relative concentration is expected to be very small and they are generally injected at very high energies (to ensure good plasma penetration), so the contribution from beam-target reactions to the total fusion power generated is expected to be small. In these conditions, it is well known that having similar amounts of D and T fuel ions leads to the optimal D-T fusion reactivity.

In many current day tokamaks and in particular in JET-ILW, the Neutral Beam ions are injected with lower energies (E=100-120keV in JET) and for large NBI power, they represent a non-negligible fraction of the core plasma ions (depending on the beam power and penetration). In these conditions, beam-target reactions can be responsible for a substantial (if not dominant) fraction of the fusion power generated and, depending on the injected beam species and the background plasma species, the optimal D:T isotope ratio for maximising fusion reactions can be fairly offset from the balanced D:T mix required in dominantly thermonuclear fusion devices. For instance, in plasmas with a significant fraction of fast Deuterium ions (D_{fast}) with E~100keV, a pure Tritium target plasma would produce more beam-target fusion reactions than a mixed D-T plasma. The inverse is also true for plasmas with large T_{fast} fractions, but the fast ion energies required for maximum fusion reactivity would be higher. This is illustrated in Fig. 1, where the D-T fusion cross-section curves for D_{fast}→T and T_{fast}→D nuclear reactions are plotted as function of the fast ion energy for each case [2]. The maximum D-T fusion cross-section is shifted from E≈110keV for fast D ions impinging onto a T target plasma to E≈165keV for the inverse case due to the isotope mass effect (i.e., due to the smaller fast ion velocities of the T ions injected at the same energy as D ions).

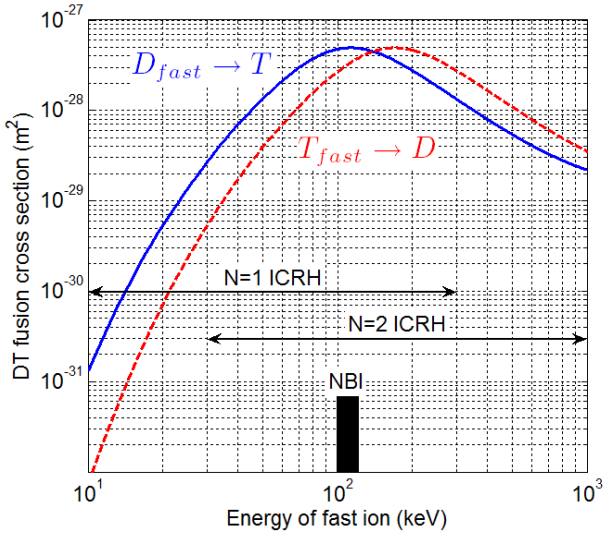

FIGURE 1. D-T fusion reaction cross-sections (Bosch & Hale) for D_{fast}→T and T_{fast}→D nuclear reactions as function of the fast ion energy. The bar shows the NB injection energy in JET (100-120keV) and the arrows indicate the approximate energy range for fundamental (N=1) or second harmonic (N=2) RF acceleration of a large minority of fuel ions.

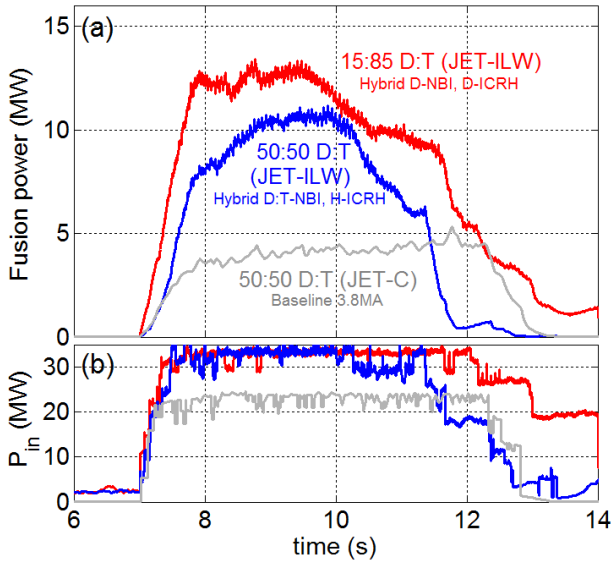

FIGURE 2. (a) D-T fusion power and (b) input power obtained in the record 50:50 D:T (#99912) and 15:85 D:T hybrid plasmas (#99972) in JET-ILW. The best stationary discharge from JET-C DTE1 (#42982) is also shown. The time vector of #42982 was shifted for a better comparison.

Since in JET-ILW the typical Neutral Beam Injection (NBI) energy is around 100-120keV (for either D or T ions), the most promising option for boosting beam-target reactions is to use Tritium rich plasmas with pure Deuterium beam injection. In addition, past experiments [3, 4] and simulations [5, 6] have shown that, among all the ICRF heating scenarios available in JET, fundamental ICRF heating of D ions is the most suitable option to accelerate one of the fuel ions to optimal energies for D-T fusion. Second harmonic ($\omega=2\omega_c$) heating of D or T ions is also possible, but a fraction of the fast ions is potentially accelerated to too high energies, thus contributing less to the overall fusion reactivity (see the horizontal arrows on Fig.1, illustrating the approximate range of ion energies generally obtained with fundamental and second harmonic ICRF heating).

Based on the arguments discussed above, a T-rich plasma scenario with D-beam injection and fundamental D ICRH was developed for the recent D-T campaign carried out in 2021 in JET-ILW [7]. It is based on hybrid plasmas at high magnetic field and moderate plasma current with relatively low core collisionality. These conditions allow

for good NBI penetration and less then 20% Deuterium in the plasma core, coming primarily from NBI fuelling but also from wall recycling, which ensures good ICRF wave absorption and optimal acceleration of the Deuterium ions.

Figure 2 compares the highest fusion performance pulses obtained in JET-ILW DTE2 with a 50:50 D:T hybrid discharge (#99912) and a 15:85 D:T hybrid discharge (#99972). Both have P_{NBI}=29MW and P_{ICRH}=4MW of input power, but the former uses mixed D:T beams and central N=1 H minority / N=2 D majority ICRH while the latter uses D_{NBI} only and fundamental (N=1) ICRH of a ~15% D minority. For comparison the best stationary discharge obtained in 1997 in JET-C (DTE1) is also shown (I_P=3.8MA, q_{95} = 3, type I ELMy H-mode plasma, #42982) [8].

The JET-ILW discharges in Fig.2 achieve high fusion power (P_{fus}>10MW and P_{fus}>12MW, respectively) but their high performance phase only lasts for a couple of seconds (3-4 α-particle slowing down times). The plasma conditions deteriorate because of core impurity accumulation, mainly driven by a gradual density peaking that reaches a critical value for neoclassical impurity screening after a few seconds. Once the temperature profile becomes hollow, a series of high order MHD modes are excited and the discharge does not recover anymore [9]. Several techniques are used in JET-ILW to mitigate core impurity accumulation in high performance discharges, such as controlling the ELM frequency for edge impurity flushing [10] or inducing core temperature peaking and density flattening with central ICRF heating [11], but the details fall outside the scope of this paper. More stationary discharges (4-5s) have also been obtained in DTE2 with slightly lower peak performance, as will be shown later. These results demonstrate that it is possible to achieve high fusion performance in a pure metallic wall environment but that additional difficulties – such as impurity control and mitigation of strong plasma-wall interaction – are an important ingredient to be considered and lead to a compromise between stationarity and performance. Nevertheless, the non-transient fusion power values achieved in JET-ILW are substantially higher than those achieved in the past with an unambiguous improvement in the fusion gain factor from $Q_{fus}=P_{fus}/P_{IN}$ = 0.18 (JET-C) to Q_{fus} = 0.32 (JET-ILW) for a 50:50 D:T plasma, where $P_{IN}=P_{NBI}+P_{ICRH}+P_{OHM}$. The higher fusion gain observed in JET-ILW is not due to the change in the plasma environment (from C to Be/W wall), but rather due to the strong ('quadratic') dependence of P_{fus} on the input power [1]. In JET, more input power means basically more NBI power which produces more ion heating and, in particular, more beam-target fusion reactions.

Another clear feature seen from Fig. 2 is that about 20% of additional fusion power can be obtained when going from a 50:50 D:T to a T-rich plasma composition with the proper NBI and ICRH settings (Q_{fus} = 0.38). Part of this improvement comes from using D-beam ions on a T-rich plasma target while another part comes from applying fundamental ICRF heating on the Deuterium ions. This paper aims on quantifying this effect and on disentangling the NBI contribution from the ICRH contribution to the fusion power enhancement. For the latter, in particular, we are interested in assessing which fraction of fusion power comes from the (thermalized) bulk D ions accelerated by ICRH and which fraction comes from the NBI+ICRH synergetic effects, the latter being expected to be small in future fusion reactors such as ITER [12]. It has to be noted that despite the higher fusion performance, the T-rich discharges exhibit lower confinement than the 50:50 D:T hybrid counterparts, not necessarily because of isotope effects, but because more gas had to be injected in the former to achieve better plasma stationarity.

The main results of the T-rich experiments followed by detailed NBI+ICRF heating modelling will be presented in this paper, highlighting the role of the different fast particle sub-species to the fusion power enhancement observed when compared to similar 50:50 D:T experiments using more standard ICRH schemes. Next, a comprehensive assessment of the impact of the isotope ratio, the NBI mixture and the ICRH scheme applied to similar hybrid D:T discharges is presented, highlighting the advantages of applying direct ICRH heating of fuel ions to the fusion performance. The paper ends with a brief summary and with future perspectives.

THE T-RICH HYBRID PLASMA

Hybrid discharges were one of the main high performance scenarios developed for the DTE2 campaign in JET [13, 14], both for 50:50 D:T and for T-rich experiments. They are characterized by a low shear q-profile in the plasma centre (obtained with a plasma current overshoot) with $q_0 \geq 1$ and large q_{95}. Relatively high normalized confinement is obtained by exploring a high β_{pol} regime, whilst keeping β_N relatively low to mitigate neoclassical tearing mode (NTM) activity. Figure 3 shows the main time traces of a high performance T-rich hybrid-like discharge (#99971). The magnetic field in the centre is B_0 = 3.85T and the plasma current (after the current overshoot) is I_P = 2.5MA (c). Around 27-29MW of Deuterium NBI ($E \approx$ 110keV) and 4MW of ICRH power is applied (a), the latter tuned for central N=1 D heating (f = 29MHz). The total radiation (e) is relatively low (P_{rad} < 10MW) and is constant throughout the discharge, suggesting that there was no significant impurity accumulation in this pulse. The ELM's are relatively small with frequency ~ 75Hz, due to a combination of high gas injection and the large connection length in the scrape-off layer ($q_{95} \approx$ 4.7). The Deuterium concentration measured by edge spectroscopy is ~15% during the flat-top phase, coming mainly from D-beam fuelling but also from wall recycling (only T_2 gas was injected in this pulse but most experiments used 50:50 D:T fuelling). The plasma density is fairly

low for a typical hybrid H-mode pulse in JET-ILW (f) while the ion and electron temperatures are large (g), with T_{i0} ≈ 12keV and T_{e0} ≈ 8keV. This leads to low core collisionality, which helps the NBI penetration (core ion heating) and enhance isotope effects in the plasma centre, such as electron/ion decoupling and fast particle turbulence stabilization [15]. Note that the ion temperature and other quantities overshoot before the start of the ELMs (t < 8s). This is part of the H-mode access strategy adopted, which is based on edge impurity screening with a high ion temperature pedestal in the ELM-free phase and a smooth transition to the type I ELMy H-mode phase by careful adjustment of the gas injection waveform and its synchronization with the high power application [16].

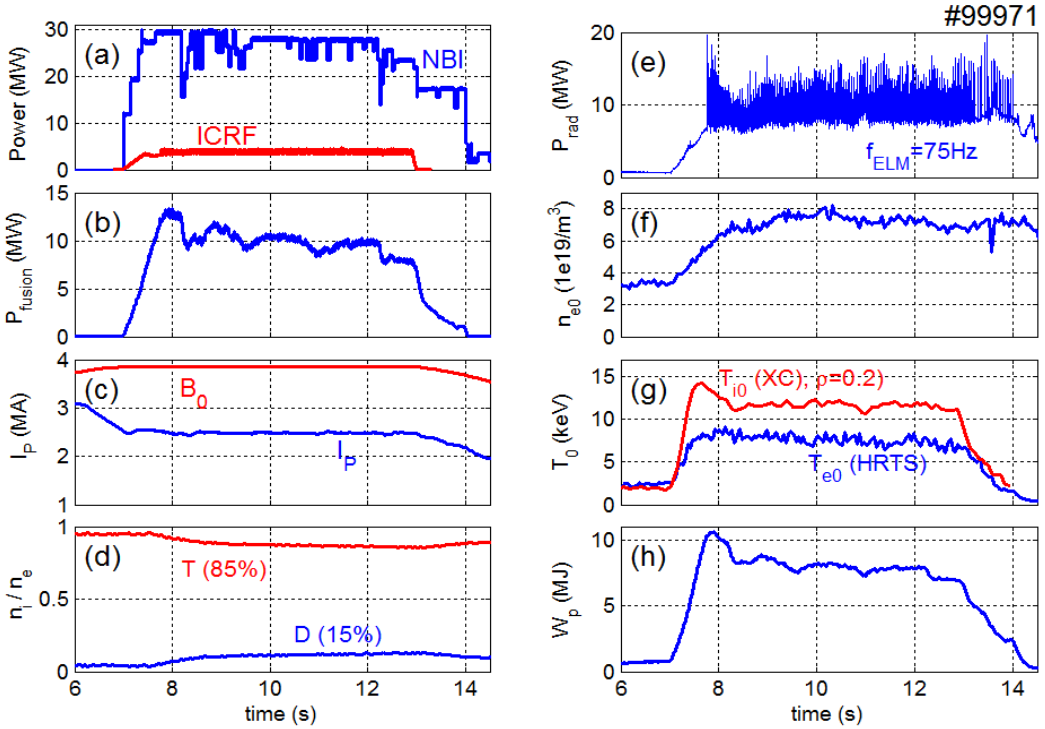

FIGURE 3: Time traces of several quantities in the T-rich hybrid pulse #99971: (a) NBI and ICRF power; (b) Fusion power; (c) Magnetic field (B_0) and plasma current (I_P); (d) D and T fuel concentrations; (e) Total radiated power; (f) Central electron density; (g) Central electron (Thomson scattering, ρ=0.1) and ion (crystal spectr., ρ=0.2) temperatures; (h) Plasma stored energy.

These conditions led to the record fusion energy and fusion power averaged over 5s (b), E_{fus}=59MJ and $<P_{fus}>$=10.1MW. Note that the fusion power time trace is strongly correlated to the input power waveform, showing that a considerable contribution of beam-target neutrons to the total fusion yield is present. As mentioned before, the 'beam'-target reactions are composed of two distinct components in these experiments, one coming from collisions between the injected D_{nbi} ions (E ≈ 110keV) and the bulk T ions and another coming from the ICRH accelerated D_{fast} ions. Actually, the D_{fast} ions accelerated by fundamental ICRH contribute to a substantial fraction of the nuclear reactions in this case, since they are accelerated to optimal energies for D-T fusion, as will be shown later.

An example of the moderate acceleration of the D ions with N=1 ICRH in a similar T-rich plasma is given in Fig.4, where the energy spectra of fast D ions measured with a neutral particle analyzer (a) in the case of NBI only and NBI + 4MW ICRH are compared (#99965). Figure 4b shows the neutron spectrum obtained with NBI + 4MW ICRH in pulse #99971 as measured by the diamond neutron spectrometer [17]. The curves show the reconstructed neutron spectra using the ion distribution functions from numerical simulations with 4MW ICRH (solid) and without ICRH (dashed), as will be discussed later. These measurements confirm that the ICRF acceleration of the D ions is restricted to relatively low energies (E<250keV) but that the number of ions in this energy range is considerable, as expected from basic RF theory for fundamental ICRF heating of large minority fractions [18].

Nevertheless, the strong impact of ICRH on various plasma quantities is clearly visible in Fig. 5: ΔP_{ICRH} = 4MW of ICRH leads to about ΔP_{fus} ≈ 3MW of extra fusion power (b), ΔT_{i0} ≈ 2keV of central ion heating (c) and ΔW_P ≈ 1MJ of additional stored energy (d). These numbers show that aside from very efficient ion heating, fundamental D ICRH has a surprisingly strong impact on the fusion power produced, with a fusion gain factor of about Q_{RF} = $\Delta P_{fus}/\Delta P_{ICRH}$ ≈ 0.7. The break-in slope analysis of the plasma stored energy (d) also suggests excellent RF heating efficiency $\eta_{RF} = \Delta\,(dW/dt) / \Delta P_{ICRH}$ [20]. Note that the η_{RF} values obtained slightly exceed 100% because of two effects: The non-thermal contribution to the stored energy signal is increased non-linearly by NBI+ICRH synergy

and, in particular, the alpha particle heating is also modulated with the ICRF power by approximately ΔP_α=0.5MW. Finally, the fact that the modulation amplitude of the various quantities remains relatively constant in the time window analyzed indicates that the Deuterium fraction in the plasma core (not measured directly) does not change much during the discharge, in agreement with the results of earlier experiments done in JET Hydrogen plasmas using D-beam heating [21, 22].

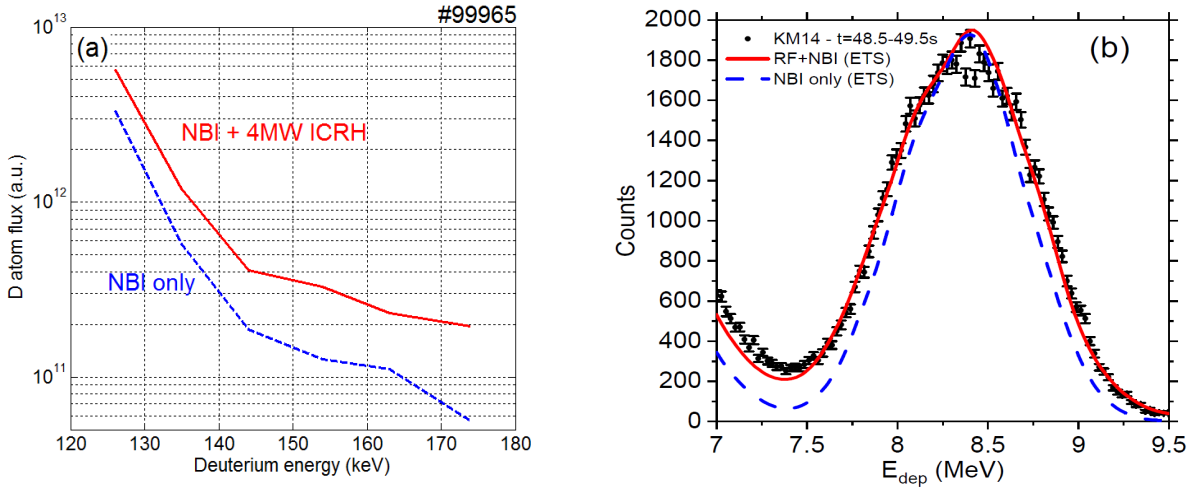

FIGURE 4: (a) Fast Deuterium energy spectra measured with the horizontal Neutral Particle Analyzer for the case of NBI only (dashed) and NBI + 4MW ICRH (solid) in a pulse with ICRH power modulation (#99965); (b) Neutron spectra measured by the vertical diamond neutron spectrometer for NBI + 4MW ICRH (#99971). The curves represent the neutron spectrum reconstructed using a specially designed synthetic diagnostic based on the Deuterium distribution functions obtained with numerical modeling of the NBI+ICRF heating with 4MW ICRH (solid) and with NBI only (dashed).

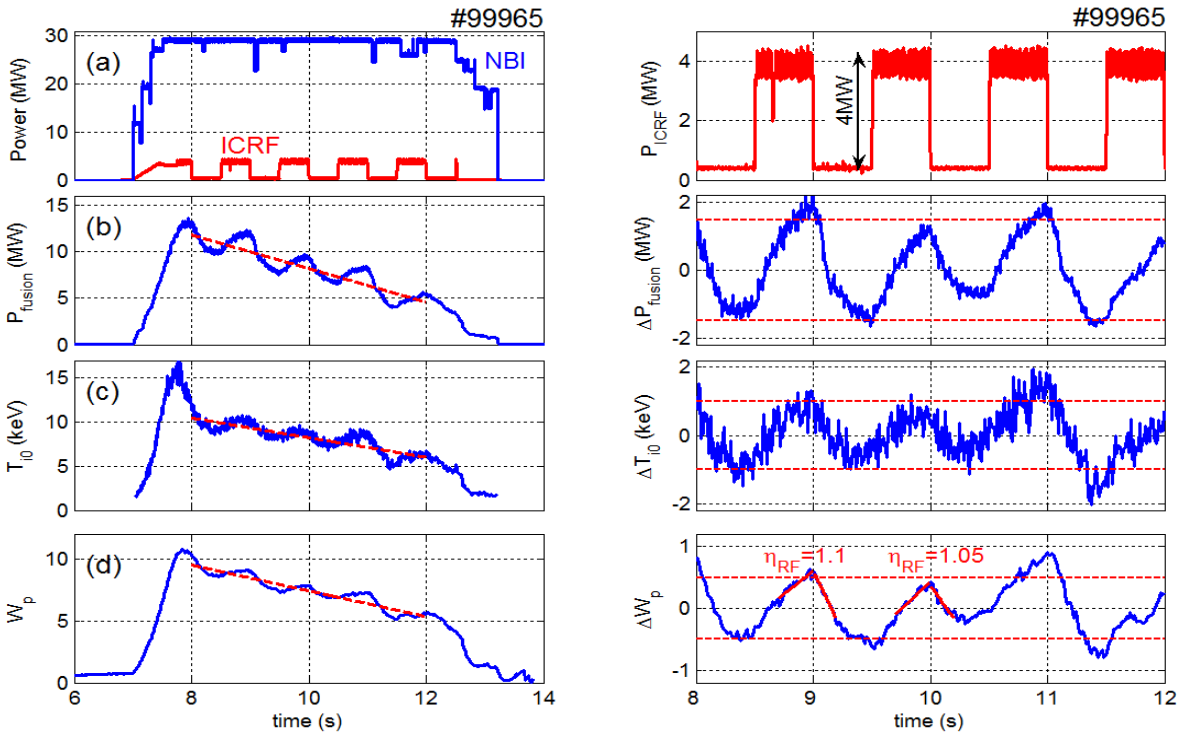

FIGURE 5: Time traces of various quantities in the T-rich hybrid pulse #99965 with a 1Hz ICRF power modulation: (a) NBI and ICRF power; (b) Fusion power; (c) Central ion temperature (charge exchange spectroscopy, ρ=0.2); (d) Plasma stored energy. The right column shows a blow-up of the same signals during the flat-top phase of the discharge, for which the average linear background values were subtracted (dashed lines on the left panel).

It may seem surprising that a modest RF acceleration of the Deuterium ions has such a strong impact on the core plasma performance and on fusion power, but the numerical simulations show that this is indeed expected because

the Deuterium RF power absorption is very peaked in the plasma centre, as will be discussed in the next sections. Predictive TRANSP simulations using the parameters of pulse #99965 also corroborate the ballpark of T_{i0} and fusion power modulation values observed in this experiment, as reported in [19].

NBI+ICRH HEATING SIMULATIONS (ETS)

The experimental parameters of pulse #99971 (Fig.3) were used to perform the NBI+ICRH heating simulations using the Heating & Current Drive (H&CD) modules available on the *European Transport Solver* (ETS) project [23,24]. The kinetic profiles were fitted from a combination of the available diagnostics data and the equilibrium was computed with a pressure constrained EFIT simulation. A radially uniform 15% Deuterium concentration was assumed, with 1% of Beryllium and 0.1% of Nickel. Alpha particles are not included. The H&CD workflow was executed as follows: First, the NBI deposition was computed using the ASCOT code [25], considering the 3 beam energy fractions as independent ion species (this is needed to correctly take into account the Doppler-shift of each beam sub-fraction in the RF heating operator). The NBI losses (reionizaton, shine-through, etc.) are discarded and only the remaining 'slowing-down' power (P_{NBI}=26.5MW) is retained in the subsequent steps. Then, the ICRH power absorption profiles for all species (including intrinsic Beryllium and the three beam energy components – modeled here as Maxwellian distributions) were computed using the 2D full wave CYRANO code [26], assuming P_{ICRH}=4MW is absorbed in the plasma and considering the main toroidal mode for dipole antenna excitation in JET ($k_{//}$=6.7m^{-1}). A simple Stix-based Fokker-Planck is used internally to calculate the converged fields in the presence of the accelerated minority species distribution. Finally, the obtained RF-fields and power absorption profiles are used as input for the Fokker-Planck code FOPLA [27], which computes the 1D distribution functions of all the ions in the plasma (including self-collisions) and the converged collisional power repartition for the given RF electric fields and RF power absorbed per species given as input. The results are summarized in Fig. 6, where the NBI source deposition and the ICRH wave power absorption profiles (left) are plotted together with the final collisional power redistribution profiles (right). The dotted lines on the right graph represent the collisional power profiles obtained with NBI only heating (P_{ICRH}=0) but otherwise identical parameters.

The ICRH absorption is very central, reaching power densities comparable to the NBI deposition despite the 5 times lower total power value (NBI=26.5MW, ICRH=4MW). The central ICRH absorption is dominated by the bulk D ions, but the D-beam ions absorb a larger amount of the RF power since they have a broader absorption profile due to their higher Doppler shift. Beryllium absorbs about 12% of the power at ~0.3m off-axis on the high-field side. The collisional redistribution in the plasma centre (right) is clearly dominated by the bulk ions (mainly T ions in this case), but some electron heating is observed near the very centre due to a combination of direct wave absorption (Landau damping / TTMP) and some fraction of slowing-down power from the highest energy D ions accelerated by ICRH. A small fraction of the power is transferred to Beryllium or stay as self-collisions on the D ions (labeled as 'other ions' in the right plot). Note that even in the absence of ICRH, ion heating is dominant in the plasma core since the beams are injected with ~110keV and the critical energy is about 150keV in these conditions.

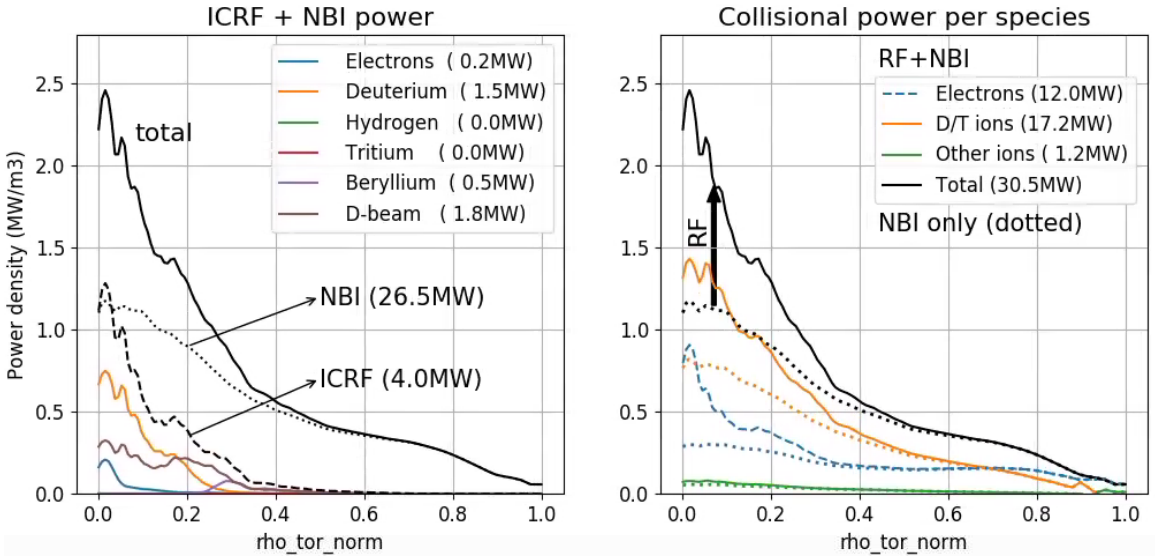

FIGURE 6: (left) ICRF wave power absorption profiles for the different plasma species for the parameters of pulse #99971, t=9s (B_0=3.85T, f=29MHz); (right) Collisional power redistribution to electrons and bulk ions considering all ions being heated in the Fokker-Planck equation. The dotted curves represent the results obtained for the NBI only case (P_{ICRH}=0).

An example of the density distribution functions ($4\pi v^2 F_0$) of the bulk Deuterium ions (left) and of the D-beam ions (right) with NBI only heating (dashed) and NBI + 4MW ICRF heating (solid) is shown in Fig.7. The distributions for the D-beam ions are summed over the 3 energy fractions (E_1=110keV, E_2=55keV, E_3=27.5keV). Consistent with the experimental measurements, the energy tails are modest (E<250keV) and the ions are accelerated within the optimal range for D-T fusion reactions (see Fig.1). For the NBI ions, a small supra-source tail is created but also part of the slowing-down population, with energies around 50-100keV, is enhanced. This is partly due to the acceleration of the E_2 and E_3 beam energy components but also due to the weaker thermalization (larger slowing down time) of the full energy beam ions when subjected to RF acceleration [5].

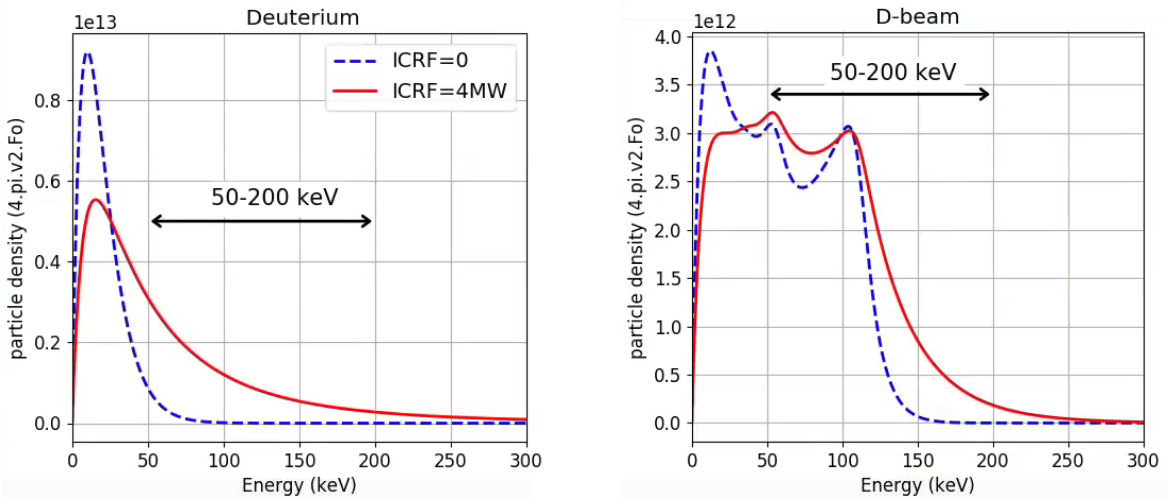

FIGURE 7: Density distributions for bulk D ions (left) and D-beam ions (right) as function of energy at ρ_{norm}=0.1 for a case without ICRH (dashed) and with 4MW of fundamental D ICRH (solid) for the plasma parameters of pulse #99971.

The set of radial distribution functions obtained for D, T and the beam ions were used to compute the D-T fusion reaction profiles, as shown in Fig.8. The neutron profiles are very peaked and the beam-target reactions are responsible for the majority (70-80%) of the D-T neutrons produced. The total fusion power with NBI+ICRH (12.3MW) is consistent with the total neutron yield measurements from the fission chamber (see Fig.3b) and the ratio between thermonuclear and beam-target reactions is also in line with preliminary analyses of the neutron spectra from various diagnostics and analysis methods [17, 28, 29]. In particular, a synthetic diagnostic of the 14MeV neutron spectra measured by the vertical diamond spectrometer using the distribution functions of the RF heated ions obtained in the simulations showed that the ICRH+NBI fast particle modeling presented here is in good agreement with the experimental data. The results are shown in Fig. 4b (solid curve).

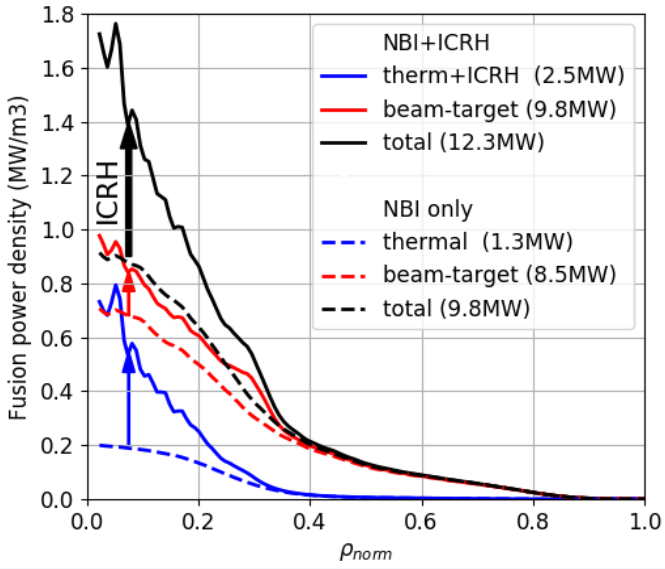

FIGURE 8: Fusion power density profiles obtained with the H&CD ETS workflow for pulse #99971 (t=9s). The dashed curves represent the results with 26.5MW of NBI-only heating while the solid curves show the results with NBI+ICRH (30.5MW).

The effect of the ICRH acceleration of the D and D-nbi ions is clear: The fusion power is increased from 9.8MW (NBI only) to 12.3MW when 4MW of ICRH is applied on top of the 26.5MW NBI power, giving an RF fusion enhancement of $\Delta P_{fus}/P_{fus}$~20% (Q_{RF}=0.6). This number is slightly lower than the results obtained from the ICRH modulation analysis shown in Fig.5 (#99965) because the temperature variation of the thermal ions is not accounted for in the modeling. Predictive transport simulations would capture this effect and show a larger RF fusion enhancement. Note that although the total fusion power being clearly dominated by beam-target reactions in this case, the RF enhancement is stronger on the thermonuclear component, since the bulk D ions distributions are more accelerated by ICRF heating than the D-beam ion distributions. Actually, this RF scheme does not rely on D-beam acceleration to produce a large D-T fusion enhancement, as will be discussed in the next section.

ISOTOPE SCAN, NBI SPECIES AND ICRH SCHEMES

The modeling tools presented in the previous section were used to study the impact of different ICRH schemes on plasmas with varying isotope concentrations and different NBI ion species. An experimental overview of the ICRH schemes tested in JET-DTE2 is given in [30]. Since these simulations were done prior to the actual JET D-T campaign, the plasma parameters of a high performance Deuterium hybrid discharge were adopted (n_{e0}=8x10^{19}/m^3, T_{e0}=10keV, T_{i0}=12keV) and the isotope concentration was scanned from a pure D to a pure T plasma, using different NB injection species and assuming a constant input power of P_{nbi}=32MW. For consistency, the kinetic profiles and the NBI parameters (beam deposition as computed for a 50:50 D:T case and source energy = 120keV) were kept constant for the scans, that is, isotope transport effects and changes in the beam deposition due to changes in the plasma and beam compositions are not accounted for. The resulting fusion power obtained as function of the D:T ratio for 3 NB injection cases are summarized in Fig.9. For each NBI case, 3 different ICRF heating schemes were simulated: Fundamental D heating with 1% Be (circles), N=2 T with 0.3% N=1 He^3 heating (squares) and N=2 D with 0.5% N=1 H ICRF heating (triangles). The minorities were included to account for the parasitic RF absorption of background minority traces, particularly important for the N=2 T and N=2 D heating scenarios, but they do not directly contribute to the fusion power in these simulations. In reality, they can also add to the RF fusion power enhancement via collisional power transfer to the bulk ions but this requires predictive transport simulations and is outside of the scope of this paper [19, 31, 32]. The small dots represent the results with NBI only heating (ICRF=0).

Because in JET a substantial part of the fusion power comes from beam-target reactions, the NBI-only curves (ICRF=0) dominate the overall fusion performance. In the mixed D:T beam case (left), the maximum fusion power is obtained around 40:60D:T and it is not very sensitive to the isotope ratio within about +/-10%. In these conditions, about half of the power is generated by thermonuclear reactions and the other half by beam-target reactions. When only D-beams are injected (middle), the maximum fusion power shifts towards the T-rich region and the total fusion power can be increased by about ~2.5MW w.r.t. the balanced D:T beam case, similar to what was observed in the experiments (see Fig.2). At D:T 20:80, about 75% of the power is produced by beam-target reactions. Even at balanced D:T ratio, the total power slightly exceeds the balanced D:T beam case in these conditions. When injecting T-beams only (right) the picture is inversed and D-rich plasmas become more attractive, but the total fusion achievable is lower than in the other cases with the injection energies available in JET (E_{nbi}<120keV).

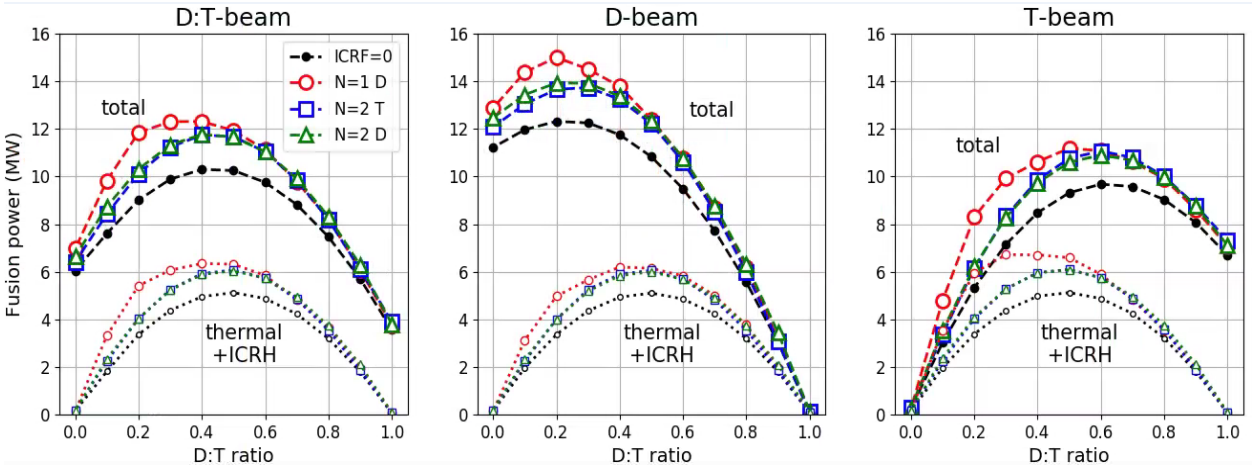

FIGURE 9: Fusion power estimates as function of the D:T isotope ratio for 3 NB injection cases (P_{NBI}=32MW, E_{nbi}=120keV) and 3 different ICRF heating schemes (P_{ICRH}=4MW): Fundamental D heating with 1% Be (circles), N=2 T with 0.3% N=1 He^3 heating (squares) and N=2 D with 1% N=1 H ICRF heating (triangles). The NBI only values (ICRF=0) are also shown (small dots).

The effect of adding 4MW of ICRH with different heating schemes is significant in all cases and is better illustrated in Fig.10, where the fusion power enhancement due to ICRH, $\Delta P_{fus} = P_{fus}$(ICRH+NBI) – P_{fus}(NBI only), is summarized. For 50:50 D:T the 3 ICRH schemes show similar results independent of the NB species injected, with a fusion power enhancement of ΔP_{fus}~1.5MW and about 2/3 of the fusion power gain coming from the enhancement of 'thermonuclear' reactions (white bars) due to ICRF acceleration of the bulk ions. The N=1 D heating scheme slightly outperforms the other 2 ICRH schemes, in particular for the T-beam case. In T-rich plasmas, the N=1 D heating scheme clearly stands out and at 20:80 D:T it produces a fusion power enhancement exceeding ΔP_{fus}~2.5MW for all NBI cases. For this heating scheme the 'thermonuclear' + ICRF contribution to the fusion power enhancement is also dominant, in particular for the D:T beam and T-beam cases, where less (or none) D-beam ions are present and a larger fraction of the RF power is absorbed by the bulk D species. The D-rich cases show the lowest fusion power enhancement for the three ICRH schemes considered (ΔP_{fus}<1MW).

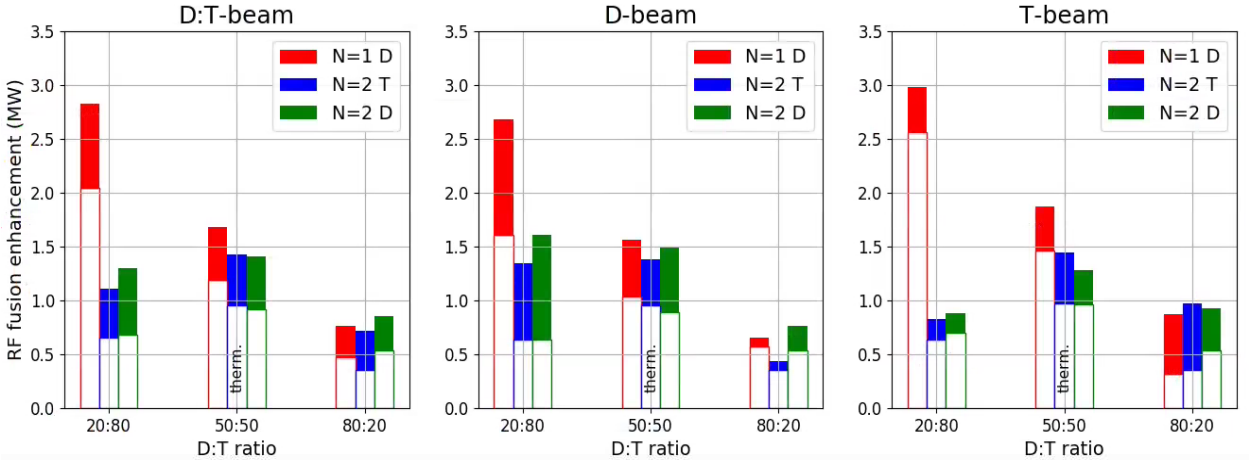

FIGURE 10: ICRF fusion power enhancement P_{fus} (ICRH+NBI) – P_{fus} (NBI only) as function of the D:T isotope ratio for 3 NB injection cases and 3 different ICRH schemes (data from Fig.9). The white part of the bars represents the contribution from the ICRH acceleration of the bulk ions ('thermonuclear') while the colored part indicates the fusion gain by NBI+ICRH synergy.

It's important to mention that the fusion enhancement for the N=2 D case and in particular for the N=2 T case may be somewhat underestimated, since they were modeled with a small minority background (0.5% H and 0.3% He^3, respectively), which can absorb a significant part of the ICRF power originally destined to the D/T fuel ions. In addition, the contribution to the bulk plasma temperature due to the additional heat sources related to the minority ion absorption is not accounted for in the interpretative simulations shown here. This could be important for the N=2 T heating case, since the accelerated He^3 ions are expected to produce collisional bulk ion heating.

SUMMARY AND CONCLUSIONS

High performance T-rich hybrid-like discharges were developed for the DTE2 experimental campaign in JET-ILW [7]. With 33MW of input power (P_{NBI}=29MW, P_{ICRH}=4MW), 10MW of fusion power was sustained for 5s (E_{fus}=59MJ) and about 12.5MW was achieved for t=2s (3-4 α-particle slowing-down times). This was obtained by boosting beam-target nuclear reactions by (i) injecting 110keV D beam ions into T-rich plasmas and (ii) using fundamental ICRF heating of the bulk and beam D ions. The latter is particularly efficient since fundamental heating of large minorities accelerates the fuel ions to optimal energies with respect to the maximum of the D-T fusion cross section, while simultaneously producing efficient bulk ion heating.

The ETS heating and current drive (H&CD) workflow [23, 24] was used to model the T-rich plasma scenario in terms of the NBI + ICRH slowing-down dynamics and the resulting D-T neutron production, which were both validated against the experimental measurements with satisfactory results. These codes were then used to assess the fusion performance optimization as function of the D:T isotope ratio, the NB injected species and the ICRH scheme applied to similar JET-ILW high performance hybrid plasmas. Without accounting for ICRH effects, it was confirmed that the best fusion performance with mixed D:T beam injection is obtained with a roughly balanced D:T mixture, with about half of the 14MeV D-T neutrons coming from thermonuclear reactions and the other half from beam-target reactions. When using D-beam injection, on the other hand, the fusion power can be enhanced by ~20% and the maximum power is observed for T-rich plasmas, with 70-80% of the neutrons coming from beam-target reactions. Adding 4MW of ICRH to 29MW of NBI power increases the fusion performance by ΔP_{fus}~15% in general (with any ICRF heating scheme), but this value is significantly larger (ΔP_{fus}≥25%) when going to T-rich

plasmas and using fundamental D heating, which drives the fuel D ions to optimal energies for D-T fusion. Actually, the RF fusion enhancement produced by N=1 D ICRH is mainly due to the acceleration of the bulk D ions and does not depend on the NBI species injected, being more efficient without D-beams, where the power is mostly directed to the bulk ions. In JET, D-beams are needed to achieve high fusion power in T-rich plasmas independently of ICRH, but in thermonuclear reactors this is not the case, making this heating scheme an attractive option for future devices such as ITER [33] or SPARC [34], where the ICRF+NBI synergy is small (or absent).

Although expected to be more efficient at low concentrations (<30%), fundamental D ICRH can also be used in balanced 50:50 D:T JET plasmas without the need of injecting any minority species [35]. In ITER, in particular, it is expected to work well at 50:50 D:T at full current and field (f=40MHz) with dominant central D absorption and some off-axis Be absorption [12]. An important aspect to be clarified is the impact of the parasitic absorption of the fusion-born alpha particles (same resonance position as the D ions). ICRF power absorption of the thermalized alpha particles (He ash) is beneficial since they will slow down onto the bulk ions, but if high energy alphas absorb power far off-axis (due to their large Doppler shift), their orbits may become too wide and produce undesired fast ion losses and enhanced plasma wall interaction. This effect is the subject of ongoing modeling research.

ACKNOWLEDGMENTS

See the author list of J. Mailloux et al., Nuclear Fusion 62, 042026 (2022) for the list of JET Contributors. This work has been carried out within the framework of the EUROfusion Consortium, funded by the European Union via the Euratom Research and Training Programme (Grant Agreement No 101052200 - EUROfusion). Views and opinions expressed are those of the author(s) and do not necessarily reflect those of the European Union or the European Commission.

REFERENCES

1. C. Maggi et al, to appear in *Nucl. Fusion* IAEA FEC 2023
2. H.-S. Bosch and G.M. Hale 1992 *Nucl. Fusion* 32 611
3. D. F. H. Start et al 1999 *Nucl. Fusion* 39 321
4. A. Krasilnikov et al 2009 *Plasma Phys. Ctrl. Fus.* 51 044005
5. E. Lerche et al 2009 *Plasma Phys. Ctrl. Fus.* 51 044006
6. L.-G. Eriksson et al 1999 *Nucl. Fusion* 39 337
7. M. Maslov et al, special *Nucl. Fusion* on JET T & DT (2023)
8. L. D. Horton et al 1999 *Nucl. Fusion* 39 993
9. G. Pucella et al 2021 *Nucl. Fusion* 61 046020
10. A. Field et al., accepted in *Nucl. Fusion* (NF-105616.R1)
11. E. Lerche et al 2016 *Nucl. Fusion* 56 036022
12. M. Schneider et al 2021 *Nucl. Fusion* 61 126058
13. J. Hobirk et al 2012 *Plasma Phys.Ctrl.Fus.* 54 095001
14. C. D. Challis et al 2022, 48th EPS Conf. on Plasma Phys. O1.101
15. J. Garcia et al 2022 *Plasma Phys. Ctrl. Fus.* 64 104002
16. J. Hobirk et al, special *Nucl. Fusion* on JET T & DT (2023)
17. M. Nocente et al 2022 Rev, of Sci. Instr. 93, 9 093520
18. T. H. Stix 1975 *Nucl. Fusion* 15 737
19. P. Mantica et al, in prep. for *Nucl. Fusion* (2023)
20. E. Lerche et al 2008 *Plasma Phys. Ctrl. Fus.* 50 035003
21. M. Maslov et al 2018 *Nucl. Fusion* 7 076022
22. M. Marin et al 2020 *Nucl. Fusion* 60 046007
23. D. Kalupin, et al 2013 *Nucl. Fusion* 53 123007
24. P. Strand et al 2018 IAEA-FEC CN-258, India, TH/P6-25
25. E. Hirvijoki et al, *Comp. Phys. Comm.* 185 (2014) 1310
26. Ph. Lamalle, PhD Thesis, LPP-ERM/KMS, Report 101, Université de Mons, Belgium (1994)
27. D. Van Eester et al 2011 *Plasma Phys. Ctrl. Fus.* 53 092001
28. C. Hellesen et al 2015 *Nucl. Fusion* 55 023005
29. D. Rigamonti et al, in prep. for *Nucl. Fusion* (2023)
30. Ph. Jacquet et al, these proceedings
31. P. Huynh et al 2021 *Nucl. Fusion* 61 096019
32. H.-Tae Kim et al, special *Nucl. Fusion* on JET T & DT (2023)
33. ITER Research Plan 2018, Technical Report ITR-18-03
34. P. Rodriguez-Fernandez et al 2022 *Nucl. Fusion* 62 042003
35. E. Lerche et al 2020, *AIP Conf. Proc.* 2254, 030007